LWT - Food Science and Technology 203 (2024) 116350

Contents lists available at ScienceDirect

LWT

journal homepage: www.elsevier.com/locate/lwt

Exploration of phenolic profile from mangosteen (*Garcinia mangostana* L.) pericarp and their contribution to inhibitory effects on α-amylase and α-glucosidase

Mengting Lai [a,b], Hongzhu Chen [a,b], Xiaozhen Liu [a,*], Fuxiang Li [c], Fengyuan Liu [a], Yuting Li [a], Jingkun Yan [a], Li Lin [a]

[a] *Engineering Research Center of Health Food Design & Nutrition Regulation, Dongguan Key Laboratory of Typical Food Precision Design, China National Light Industry Key Laboratory of Healthy Food Development and Nutrition Regulation, School of Life and Health Technology, Dongguan University of Technology, Dongguan, 523808, China*

[b] *College of Food Science, South China Agricultural University, Guangzhou, 510642, China*

[c] *Dongguan University of Technology Analytical and Testing Centre, Dongguan, 523808, China*

ARTICLE INFO

Keywords:
Mangosteen (*Garcinia mangostana* L.) pericarp
Phenolic profile
Gradient ethanol elution
α-amylase
α-glucosidase

ABSTRACT

The aim of this study was to reveal the phenolic profile of mangosteen (*Garcinia mangostana* L.) pericarp and investigate their inhibitory effects on α-amylase and α-glucosidase. Mangosteen pericarp polyphenols (MPP) obtained by acetone extraction were fractionated with gradient ethanol elution. A total of twenty nine phenolic chemicals were found and quantified by UPLC-Q-TOF-MS/MS. MPP eluted by the 60% ethanol solution ($MPP_{60\%}$) showed the highest total phenolic content. Moreover, $MPP_{60\%}$ displayed the greatest inhibition activities on α-amylase and α-glycosidase by competitive and mixed inhibitions. Mechanistically, the inhibitory effects of $MPP_{60\%}$ on α-amylase and α-glucosidase involved the changes of the secondary structure as well as the static fluorescence quenching of these enzymes. Pearson correlation coefficients revealed that procyanidin B2, quercetin glucoside, and mangostain contributed most to inhibiting the activities of α-amylase and α-glucosidase. This study indicated that polyphenols from mangosteen pericarps can be developed into potential inhibitors of α-amylase and α-glucosidase, offering a viable strategy for the valorization of mangosteen pericarps.

1. Introduction

With the changes in people's lifestyles and dietary structure, the incidence of type 2 diabetes caused by obesity was increasing year by year. Diabetes and its complications had emerged as a significant worldwide public health issue, it was considered as the third major non-communicable chronic disease threatening human health after tumors and cardiovascular diseases (Tinajero & Malik, 2021). Based on estimates from the International Diabetes Federation, the number of adults (aged 20–79) with diabetes worldwide was 537 million in 2021 and is expected to reach 783 million by 2045 (Sun et al., 2022; Yan et al., 2022). Numerous studies have demonstrated a strong correlation between persistent postprandial hyperglycemia and the establishment of type 2 diabetes. Therefore, effectively reducing postprandial blood glucose levels has become a key component of diabetes treatment.

Alpha (α)-amylase and α-glucosidase are the most important enzymes in human glucose metabolism. Alpha-amylase hydrolyzes the α-(1, 4)-D-glycosidic bonds of starch or other glucose polymers in the digestion process of carbohydrates (Janeček et al., 2014), while α-glucosidase cleaves the glycosidic bond of the oligosaccharides that liberate glucose as the final digestive product (Hossain et al., 2020; Zhang et al., 2020). Thus, inhibitors for α-amylase or α-glucosidase played a significant role in combating diabetes. Acarbose and voglibose, the main drugs for the treatment of diabetes, could effectively inhibit the level of postprandial blood glucose, while side effects including nausea, vomiting, flatulence, renal dysfunction as well as drug resistance had been frequently reported with long-term use. Natural compounds from plant resources with attractive safety property are intensively explored as inhibitors of these key digestive enzymes.

A broad class of chemicals known as polyphenols have at least one aromatic ring along with one or more hydroxyl groups and other substituents. Based on their chemical structures, polyphenols can be categorized into numerous classes, including lignans, stilbenes, flavonoids,

* Corresponding author. School of Life and Health Technology, Dongguan University of Technology, Dongguan, 523808, China.
E-mail address: liuxz@dgut.edu.cn (X. Liu).

https://doi.org/10.1016/j.lwt.2024.116350
Received 22 March 2024; Received in revised form 12 June 2024; Accepted 13 June 2024
Available online 14 June 2024

Abbreviation

α	alpha
β	beta
CD	circular dichroism
γ	gamma
ESI	electrospray ionization
IC_{50}	half maximal inhibitory concentration
MP	mangosteen pericarps
MPP	mangosteen pericarp polyphenols
$MPP_{20\%}$	MPP eluted by the 20% ethanol solution
$MPP_{40\%}$	MPP eluted by the 40% ethanol solution
$MPP_{60\%}$	MPP eluted by the 60% ethanol solution
$MPP_{80\%}$	MPP eluted by the 80% ethanol solution
PAHBAH	*para*-hydroxybenzoic acid hydrazide
PBS	phosphate-buffered saline
pNPG	4-Nitrophenyl-β-D-glucopyranoside
Q-TOF-MS	quadrupole time-of-flight mass spectrometry
SD	standard deviation
TPC	total phenolic content
UPLC	ultra-high performance liquid chromatography

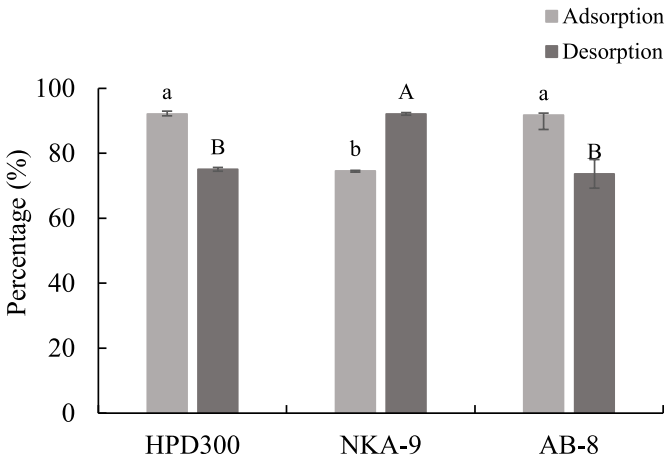

Fig. 1. Adsorption and desorption rates of polyphenols in three different resins. Different letters indicated significant differences in adsorption or desorption ($P < 0.05$).

and phenolic acids (Croft, 2016; Karas et al., 2016). To date, more than 8000 polyphenols have been found in plant-related products, such as coffee, tea, olive oil, fruits, vegetables, wine, nuts, beans, and whole grains. Polyphenols have attracted great attention for their effective antioxidant properties and protective roles against tumor growth, neurodegenerative conditions, diabetes, etc (Cao et al., 2018; Luca et al., 2020; Stefek, 2011; Xiao & Högger, 2015). Numerous epidemiological and nutritional evidences suggested that natural dietary polyphenols exerted the ability to inhibit α-amylase and α-glucosidase (Papoutsis et al., 2021). However, the polyphenols reported previously were mainly crude extracts from plant sources, besides, the underlying inhibition mechanisms remain elusive. Therefore, fractionation of the crude extracts is recommended to prepare the phenolic compounds with inhibition activities on α-glucosidase and α-amylase, as it may help to clarify the contribution of each class of bioactive compounds to inhibit these enzymes activities.

Mangosteen (*Garcinia mangostana* L.) is an inter-hybrid fruit, native to Malaysia and Indonesia, now mainly distributed in Southeast Asian countries and cultivated in Guangdong, Hainan, Fujian, Taiwan, and other provinces in China. The use of mangosteen in the food processing industry for fruit wine, preserves, jams, purées and other products produced a large number discard of pericarps. Mangosteen pericarps (MP), riched in pectin, crude fiber and polyphenols, were 60% of the fresh weight of a single fruit, and they had a certain role in antioxidant, anti-inflammatory, anti-bacterial and anti-cancer (Lim et al., 2020; Wihastuti et al., 2019). In Southeast Asia, mangosteen pericarps were used as a folk medicine to treat suppuration, chronic ulcers, infected wounds, diarrhea, and dysentery. Mangosteen peel infusion was reported to ameliorate the liver and kidney's histological structures and function in H_2O_2 induced rats (Rusman et al., 2021). Ghasemzadeh and colleagues found that α-mangostin obtained with microwave-assisted extraction from mangosteen pericarp exhibited high antibacterial activity, particularly against Gram-positive bacteria (Ghasemzadeh et al., 2018). However, the phenolic profile of mangosteen pericarp and their potential anti-diabetic activity still not be fully illuminated. Thus, the phenolic profile of mangosteen pericarp was explored by gradient ethanol elution and UPLC-Q-TOF-MS/MS. Moreover, the inhibition activities of mangosteen pericarp polyphenols (MPP) on α-amylase and α-glucosidase, as well as the contribution of each phenolic component to the inhibitory effects were revealed in this study.

2. Materials and methods

2.1. Reagents and chemicals

Ethanol, acetone, and concentrated hydrochloric acid were supplied from Fuyu Co., Ltd. (Tianjin, China). Glacial acetic acid, sodium hydroxide, and 4-hydroxybenzoyl hydrazide were supplied by Macklin Biochemical Technology (Shanghai, China). Anhydrous sodium carbonate was purchased from Aladdin Biochemical Technology (Shanghai, China). Formic acid, acetonitrile, quercetin, catechin, *p*-hydroxybenzoic acid, rutin, cornflower-3-*O*-glucoside, luteolin, gallic acid, epicatechin, *p*-coumaric acid, procyanidin B2, α-mangostin, salicylic acid (≥98% purity by HPLC), α-amylase (porcine pancreas), and α-glucosidase (*Saccharomyces cerevisiae*) were obtained from Sigma-Aldrich (Saint Louis, MO, USA). 4-Nitrophenyl-β-D-glucopyranoside (*p*NPG) was supplied by Yuanye Biotechnology Co., Ltd. (Shanghai, China).

2.2. Phenolic compounds extraction

Mangosteen pericarps (10.0 g) were homogenized with 80% frozen acetone (50 mL) for 3 min with an ice bath and then centrifuged with 1200×*g* for 10 min to collect the supernatants. The extraction process was repeated three times. The combined supernatants were evaporated and then mixed with 30 mL of acetone containing 0.1% acetic acid followed by filtering with 0.45 μm nylon filter membrane. Finally, the MPP were obtained and then stored in a −80 °C refrigerator for further analysis.

2.3. Static adsorption and desorption test

Three different types of macroporous resins, namely HPD300, AB-8, and NKA-9, were applied to purify phenolic compounds. Firstly, the macroporous resins were soaked in ethanol for 24 h followed by rinsing with pure water. After soaking in 1.4 1.4 mol/L HCl and 0.5 mol/L NaOH for 4 h, the resins were washed with deionized water to bring their pH down to neutral. The static adsorption as well as desorption of phenolic compounds was performed as follows:

Static adsorption test: Accurately weighed 1.000 g of each resin to 30 mL of phenolic compounds extract in the dark conditions, oscillated with 100 r/min at 25 °C for 24 h, then determined the phenolic content of the supernatant. Calculated the adsorption rate (%) as Eq (1):

$$\text{Adsorption rate } (\%) = \frac{C_0 - C_1}{C_0} \times 100 \quad (1)$$

Table 1
Quantitative analysis of phenolic constituents in mangosteen pericarps.

Phenolic component category	Phenolic components	Content of identified component (μg/g elution)				
		MPP (μg/g extract)	$MPP_{20\%}$	$MPP_{40\%}$	$MPP_{60\%}$	$MPP_{80\%}$
Procyanidins	procyanidin B1	4114.85 ± 455.03	15545.03 ± 2469.30	6598.60 ± 322.62	9402.60 ± 341.62	7987.22 ± 165.55
	procyanidin B2	24796.86 ± 2271.85	788.99 ± 182.46	41736.88 ± 1183.98	44309.87 ± 1047.59	48508.93 ± 1687.71
Flavanols	catechin	21561.79 ± 1175.67	22513.83 ± 2235.59	29117.06 ± 927.17	30020.74 ± 1479.85	32179.39 ± 941.03
	epicatechin	295.46 ± 32.60	662.04 ± 81.79	4.26 ± 0.18	457.07 ± 149.74	526.05 ± 32.16
	dihydroquercetin (quercetin equivalents)	114.16 ± 10.39	160.77 ± 9.33	175.94 ± 2.08	27.91 ± 0.75	222.32 ± 12.46
	quercetin glucoside	139.51 ± 11.49	24.39 ± 6.53	230.29 ± 7.48	385.37 ± 8.16	301.31 ± 14.91
	rutin	826.57 ± 75.22	–	1497.09 ± 88.23	2367.51 ± 126.29	1784.25 ± 124.36
Phenolic acids	salicylic acid	0.27 ± 0.09	2.31 ± 0.33	0.95 ± 0.11	4.51 ± 0.04	1.08 ± 0.11
	gallic acid	18.30 ± 2.04	22.88 ± 4.59	57.39 ± 4.68	65.07 ± 9.39	55.83 ± 7.01
	coumarin acid	–	58.88 ± 2.77	–	–	–
Anthocynidins	cyanidin	166.48 ± 28.35	2726.33 ± 640.60	96.67 ± 17.64	467.87 ± 33.02	148.69 ± 9.31
Flavonoids	luteolin	46.66 ± 8.37	–	84.11 ± 3.21	150.78 ± 8.17	117.03 ± 13.90
Xanthones	α-mangostin	8615.93 ± 4613.02	79.71 ± 11.90	16.46 ± 1.64	41.52 ± 5.44	36.01 ± 0.08
	β-mangostin	79.89 ± 40.48	8.97 ± 0.17	–	8.85 ± 0.11	–
	garcinone C	12.17 ± 0.45	50.33 ± 7.94	15.81 ± 0.42	13.85 ± 4.16	17.62 ± 0.71
	mangostanin	15.07 ± 0.37	9.85 ± 0.13	9.24 ± 0.54	20.96 ± 0.31	9.39 ± 0.21
	garcinoxanthone D or E	25.27 ± 4.64	–	–	42.61 ± 0.15	27.51 ± 1.10
	9-hydroxycalabaxanthone or garcimangosone B	37.77 ± 15.90	8.39 ± 0.29	8.28 ± 0.10	–	–
	1,3,7-trihydroxy-2-(3-methylbut-2-enyl) -xanthone	92.38 ± 47.01	6.69 ± 0.06	–	–	–
	1,7-dihydroxy-2-(3-methylbut-2-enyl) -3-methoxyxanthone	89.33 ± 40.71	6.62 ± 0.04	–	–	–
	garcinone E or 4′,5′-dihydro-1,3,6-trihydroxy-6′,6′-dimethyl-2,5-bis(3-methylbut-2-en-1-yl)pyrano [2′,3′:7,8] xanthone	477.69 ± 289.87	16.18 ± 0.28	9.43 ± 0.11	14.90 ± 0.10	9.66 ± 0.15
	1,3,6,7-tetrahydroxy-8-prenylxanthone	–	17.00 ± 3.42	14.24 ± 0.33	14.36 ± 3.89	15.41 ± 0.38
	1,3,8-trihydroxy-2-(3-methyl-2-butenyl) -4-(3-hydroxy-3-methylbutanoyl)-xanthone or 1,2-dihydro-1,8,10-trihydroxy-2-(2-hydroxypropan-2-yl) -9-(3-methylbut-2-enyl) furo [3,2-α] xanthen-11-one	138.01 ± 29.30	8.50 ± 0.28	8.00 ± 1.30	13.18 ± 0.29	22.37 ± 10.07
	γ-mangostin	17.18 ± 1.79	60.74 ± 6.57	28.98 ± 1.21	30.19 ± 1.15	32.88 ± 2.63
	cudraxanthone G	13.74 ± 1.32	–	–	22.27 ± 0.29	14.96 ± 0.48
	7-*O*-methylgarcinone E, mangostanaxanthones II or parvifolixanthone C	2738.35 ± 687.41	34.99 ± 6.03	10.76 ± 1.10	11.54 ± 0.11	13.68 ± 0.78
	garcimangosxanthone F	9.20 ± 0.41	9.49 ± 0.18	9.67 ± 0.23	8.97 ± 0.31	9.11 ± 0.34
	garcimangosxanthone G	12.42 ± 2.37	–	–	–	–
	calocalabaxanthone	12.76 ± 2.05	–	–	–	–
		29.55 ± 10.49	–	–	–	–
		17.52 ± 0.58	17.18 ± 0.48	17.82 ± 1.25	20.81 ± 0.52	19.45 ± 1.36

Notes: MPP, polyphenols extracted with 80% frozen acetone from mangosteen pericarp; $MPP_{20\%}$, MPP eluted by the 20% ethanol solution; $MPP_{40\%}$, MPP eluted by the 40% ethanol solution; $MPP_{60\%}$, MPP eluted by the 60% ethanol solution; $MPP_{80\%}$, MPP eluted by the 80% ethanol solution.
Correction factors for quercetin glucoside; β-mangostin, garcinone C; mangostanin, garcinoxanthone D or E; 9-hydroxycalabaxanthone or garcimangosone B; 1,3,7-trihydroxy-2- (3-methylbut-2-enyl) -xanthone; 1,7-dihydroxy-2-(3-methylbut-2-enyl)-3-methoxyxanthone; garcinone E or 4′,5′-dihydro-1,3,6-trihydroxy-6′,6′-dimethyl-2,5-bis (3-methylbut-2-en-1-yl) pyrano [2′,3′:7,8] xanthone; 1,3,6,7-tetrahydroxy-8-prenylxanthone; 1,3,8-trihydroxy-2- (3-methyl-2-butenyl) -4- (3-hydroxy-3-methylbutanoyl) -xanthone or 1,2-dihydro-1,8,10-trihydroxy-2- (2-hydroxypropan-2-yl) -9- (3-methylbut-2-enyl) furo [3,2-α] xanthen-11-one; γ-mangostin; cudraxanthone G; 7-*O*-methylgarcinone E; mangostanaxanthones II or parvifolixanthone C; garcimangosxanthone F; garcimangosxanthone G; and calocalabaxanthone were 1.54, 1.03, 1.01, 1.04, 1.08, 0.99, 0.76, 0.79, 1.13, 0.80, 1.01, 0.97, 0.96, 1.17, 1.17, 1.17, and 2.0, respectively.

C_0 and C_1 represented the initial and the final concentrations of phenolic compounds in the adsorption experiment (mg/mL), respectively.

Static desorption test: The resins that had fully adsorbed phenolic compounds in the static adsorption test were washed and dried, then 60% ethanol solution was added to oscillate with low speed in a clean shaking bottle, the phenolic content in the supernatant was measured per 60 min, and the desorption rate (%) was calculated as Eq (2):

$$\text{Desorption rate}\ (\%) = \frac{C_2}{C_0 - C_1} \times 100 \quad (2)$$

C_0 and C_1 represented the initial and the final concentrations of phenolic compounds in the adsorption experiment (mg/mL); C_2 was the concentration of phenolic compounds in the desorption solution (mg/mL).

Table 2
The IC_{50} values for inhibition activity of mangosteen pericarp phenolics on α-amylase and α-glycosidase.

	IC_{50} (μg/mL)					
	MPP	$MPP_{20\%}$	$MPP_{40\%}$	$MPP_{60\%}$	$MPP_{80\%}$	Acarbose
α-amylase	362.56 ± 4.44^{c}	2023.05 ± 9.97^{f}	504.20 ± 16.83^{d}	290.10 ± 4.94^{b}	1376.99 ± 53.69^{e}	49.94 ± 2.70^{a}
α-glycosidase	7.81 ± 0.69^{a}	31.14 ± 1.78^{d}	6.11 ± 0.07^{a}	6.20 ± 0.15^{a}	15.21 ± 1.20^{b}	53.35 ± 5.44^{c}

Data were showed as mean ± SD. Different letters indicated significant differences in the same row ($P < 0.05$).

2.4. Purification of phenolic compounds

The purification of phenolic compounds was performed as described with slight modifications (Li et al., 2017b). The crude extracts were dissolved in acidified acetone (acetone/acetic acid, 99.9/0.1, v/v) and loaded on an HPD300 column with a ratio of 1 g phenolic compounds per 100 g of filler. Impurities were eliminated using distilled water at a flow rate of 1.0 mL/min. After that, the adsorbed phenolic compounds were eluted using 20%, 40%, 60%, and 80% (v/v) of ethanol containing 0.1% HCl. The four eluents were evaporated and vacuum freeze-dried respectively. Then, the Folin-Ciocalteu method was employed to calculate the total phenolic content (TPC) of the eluted fractions, with gallic acid serving as the reference (Zheng et al., 2017). The TPC was given in mg of gallic acid equivalents (GAE)/g of fraction.

2.5. Qualitative and quantitative analysis by UPLC-Q-TOF-MS/MS

Phenolic components were analyzed using the ultra-high performance liquid chromatography (UPLC)-quadrupole time-of-flight mass spectrometry (Q-TOF-MS) coupled with the electrospray ionization (ESI) source. The chromatographic separation procedure was performed on the ExionLC™ system (AB Sciex, USA) with ACQUITY UPLC BEH HILIC column (2.1 × 100 mm, 1.7 μm, Waters Corp., Milford, MA, USA). 0.1% formic acid in ultrapure water (mobile phase A) and acetonitrile (mobile phase B) served as the mobile phase. The solvent gradient was as follows: 5% B for 0–1 min; 5–65% B for 1–6 min; 65–100% B for 6–18 min; 100-5% B for 18–20 min; and 5% B for 20–25 min. The injection volume was 2 μL. The flow rate was 0.25 mL/min and the column temperature was 35 °C. The AB Sciex X500R Q-TOF-MS equipped with ESI was operated in negative ion mode. The nitrogen used as the curtain gas (35 psi), the air used as the nebulizer gas and turbo gas (55 psi), the collision energy (CE) was −10 V, and the declustering potential voltage was −100 V. The scanning range was from 100 to 1100 mass-to-charge ratio, and the heater temperature was 600 °C. UPLC-Q-TOF/ESI-MS data was analyzed by SCIEX OS Software (ver 1.8) (AB Sciex, USA).

Peak area integral was applied for quantification. Reference compounds, structurally similar compounds, or compounds from the same subclass (adjusted by molecular weight) were used to generate calibration curves (Chandra et al., 2001), including procyanidin B2 (for procyanidins), quercetin (for quercetin and quercetin-based flavonols), rutin, catechin, epicatechin, gallic acid, salicylic acid, coumarin, cyanidin, luteolin, and α-mangostin (for α-mangostin and other xanthones). Calibration curves were obtained from different concentrations (0.002, 0.02, 0.2, 2.0, 20.0 μg/mL) of standard, y (procyanidin B2) = 672372x-16046.96, R^2 = 0.993; y (catechin) = 1309460x-962.38, R^2 = 0.999; y (epicatechin) = 1508590x-4997.46, R^2 = 0.999; y (rutin) = 1604220x-25669.47, R^2 = 0.998; y (quercetin) = 4399530x+2206.38, R^2 = 0.992; y (salicylic acid) = 90721.7x-302.09, R^2 = 0.999; y (gallic acid) = 481008x+583.35, R^2 = 0.994; y (*p*-coumarin acid) = 668793x+382.66, R^2 = 0.996; y (cyanidin) = 451459x-7326.98, R^2 = 0.998; y (luteolin) = 6187800x+151303.00, R^2 = 0.998; y (α-mangostin) = 5663060 x-45874.70, R^2 = 0.999. The findings were presented in terms of μg/g of eluate.

2.6. Inhibition assay of α-amylase and α-glucosidase

The inhibitory effect of MPP or ethanol-eluted fractions on α-amylase was assessed based on the method described previously (Chen et al., 2019). Briefly, normal maize starch (1 mg/mL) was prepared in 20 mL of phosphate-buffered saline (PBS), boiled at 100 °C for 30 min with inhibitor (0–2.5 mg/mL) present, then incubated at 37 °C in a water bath with mixing. For each dispersion, 1 mL of α-amylase (0.48 U/mL) was applied. After 4, 8, and 12 min, starch samples (300 μL) were collected and combined with 1.2 mL of 0.3 mol/L Na_2CO_3 solution to halt the reaction. After that, these samples were centrifuged for 5 min at 1500×*g* to remove the unreacted inhibitor and starch. The *p*-benzoic acid hydrazide (PAHBAH) technique was applied for the determination of reducing sugar content (Sun et al., 2016). The slope of a plot showing reducing sugar concentration against time was used to calculate the initial reaction velocity (v). In the assay, the inhibition percentage (%) was calculated using Eq (3):

$$\text{Inhibition percentage}\ (\%) = \left(1 - \frac{v}{v_0}\right) \times 100 \tag{3}$$

where v and v_0 were the initial reaction velocities in the system with or without inhibitor.

The inhibitory assay of α-glucosidase was performed according to Zhang et al. (2016). Briefly, 100 μL of α-glucosidase (0.5 U/mL) was mixed thoroughly with MPP or the ethanol-eluted fractions, and then incubated at 37 °C for 10 min. Then 500 μL of *p*NPG (5 mM) was incorporated into the mixture, after an extra 10 min of incubation, the absorbance was measured at 405 nm. The inhibition percentage (%) was obtained using Eq (4):

$$\text{Inhibition percentage}\ (\%) = \left(1 - \frac{A_i - A_b}{A_0}\right) \times 100 \tag{4}$$

Where A_0 and A_i are the absorbance in the system with or without inhibitor. A_b is the absorbance of the sample without *p*NPG solution. Acarbose was used as positive control.

2.7. Inhibition kinetic analysis

Inhibition kinetics were determined based on the method of inhibition assay. Maize starch and *p*NPG with a concentration of 5, 10, 15, 20 and 25 mg/mL were used as substrates for α-amylase and α-glucosidase. The catalytic rate of α-amylase or α-glucosidase to substrates was measured in the presence of various amounts of MPP eluted by the 60% ethanol solution ($MPP_{60\%}$), then the inhibition kinetic was analyzed by Lineweaver-Burk plot. Dixon plot (Eq. (5)) was used to determine competitive inhibition constant K_{ic} and Cornish-Bowden plot (Eq. (6)) was applied to obtain uncompetitive inhibition constant K_{iu} (Eisenthal & Cornish-Bowden, 1974).

$$v = \frac{V_{max}\alpha}{K_m\left(1 + \frac{i}{K_{ic}}\right) + a\left(1 + \frac{i}{K_{iu}}\right)} \tag{5}$$

$$\frac{v}{a} = \frac{V_{max}}{K_m\left(1 + \frac{i}{K_{ic}}\right) + a\left(1 + \frac{i}{K_{iu}}\right)} \tag{6}$$

The K_{ic} was the absolute vaue of the intersection points of the abscissa in Dixon plot, and the K_{iu} was the absolute vaue of the intersection points of horizontal coordinates in Cornish-Bowden plot.

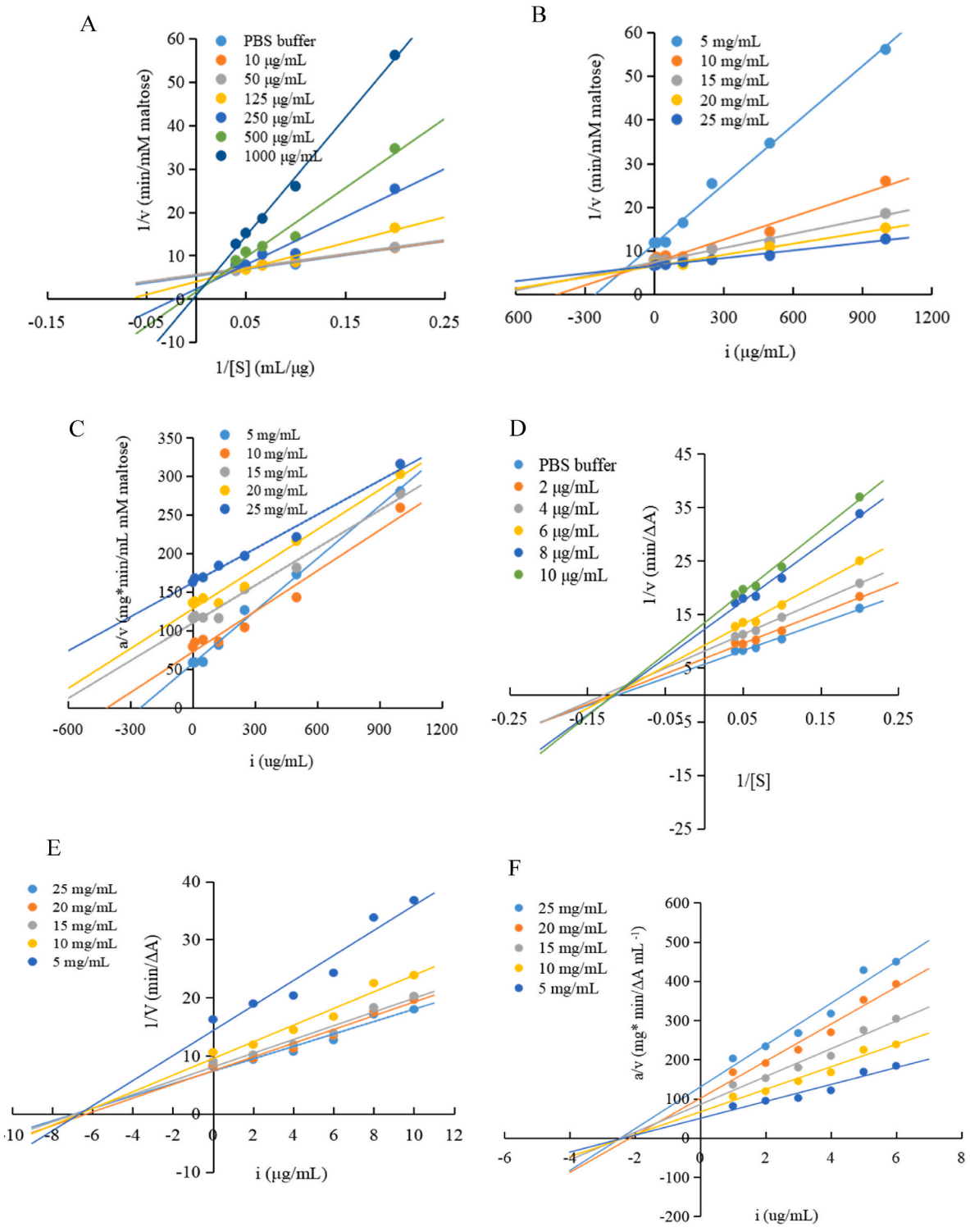

Fig. 2. Inhibition kinetic of $MPP_{60\%}$ against α-amylase and α-glucosidase. (A) Lineweaver–Burk plots of $MPP_{60\%}$ for α-amylase. (B) Dixon plots of $MPP_{60\%}$ for α-amylase. (C) Cornish-Bowden plots of $MPP_{60\%}$ for α-amylase. (D) Lineweaver–Burk plots of $MPP_{60\%}$ for α-glucosidase. (E) Dixon plots of $MPP_{60\%}$ for α-glucosidase. (F) Cornish-Bowden plots of $MPP_{60\%}$ for α-glucosidase.

2.8. Circular dichroism spectroscopy analysis

The circular dichroism (CD) spectra for the complexes of α-amylase/α-glucosidase with $MPP_{60\%}$ was obtained using Chiracan V100 spectrophotometer (Applied Photophysics Ltd., England). The spectra were acquired in the far-UV range (190–260 nm) at a response time of 1 s, a path length of 1.0 mm, and a scan speed of 100 nm/min. For every spectrum, three scans were accumulated. The α-amylase (0.48 U/mL) was individually incubated with 0, 50, 100, 125, 150, 200 and 250 μg/mL of $MPP_{60\%}$, and α-glucosidase (0.50 U/mL) was individually incubated with 0, 1, 2, 3, 4, 5 and 6 μg/mL of $MPP_{60\%}$ at 37 °C for 15 min. The CD spectrogram data was quantitatively analyzed by CDNN software.

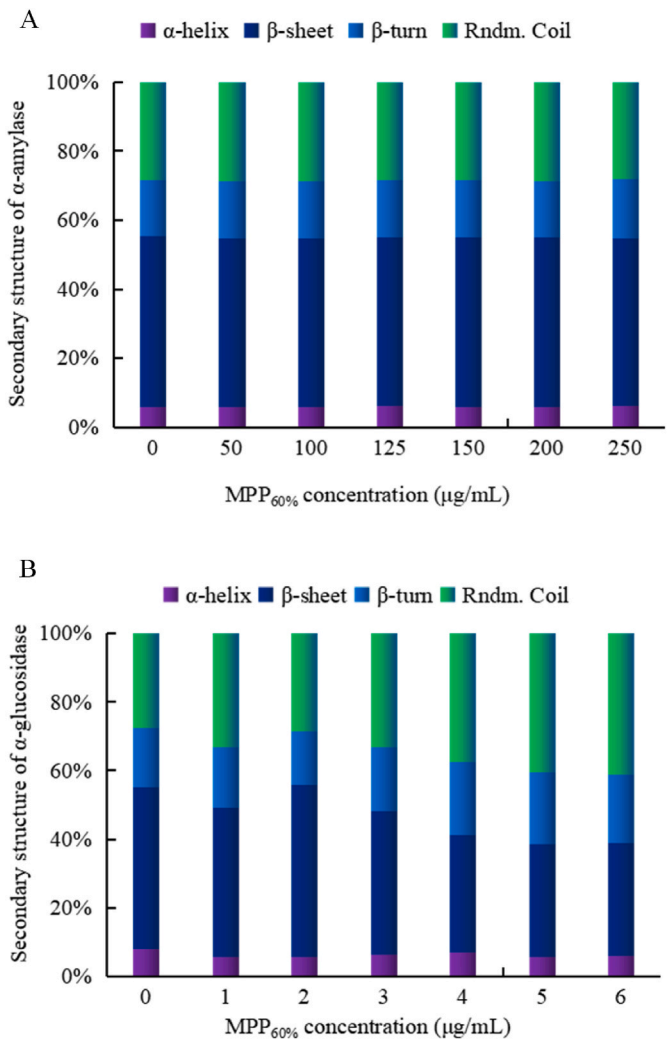

Fig. 3. Effects of $MPP_{60\%}$ on the secondary structure of α-amylase and α-glucosidase. (A) α-amylase, (B) α-glucosidase.

2.9. Fluorescence quenching

Specific amounts of α-amylase or α-glucosidase were incubated with 0.3 mL of $MPP_{60\%}$ for 5 min at three temperatures (277.15 K, 298.15 K, and 310.15 K). The fluorescence was measured using a fluorescence spectrophotometer with an excitation wavelength of 280 nm and an emission wavelength of 300–400 nm. Values of fluorescence quenching constant (K_q) and the Stern–Volmer quenching constant (K_{sv}) were obtained through the following,

$$F_0/F = 1 + K_q\tau_0[Q] = 1 + K_{sv}[Q] \quad (7)$$

where F_0 and F represented the fluorescence intensities of enzymes in the absence and presence of $MPP_{60\%}$; K_q was the bimolecular quenching constant; τ_0 was the lifetime of the fluorophore without quencher, for α-amylase, $\tau_0 = 2.97 \times 10^{-8}$ ns (Prendergast et al., 1983), for α-glucosidase, $\tau_0 = 1 \times 10^{-8}$ ns (Han et al., 2023); [Q] represented the quencher concentration, and K_{sv}, the Stern–Volmer quenching constant, was equivalent to $K_q\tau_0$. $L{\cdot}mg^{-1}$ and $L{\cdot}mg^{-1}\ s^{-1}$ were utilized as units of K_{sv} and K_q, respectively, to identify the type of fluorescence quenching, due to the molecular weights of $MPP_{60\%}$ being unknown.

2.10. Statistical analysis

Data was displayed as the mean ± standard deviation (SD). Statistical significance was analyzed through one-way ANOVA followed by the Duncan's test using SPSS 27.0 software. In addition, the Pearson correlation coefficients were carried out using SPSS. Comparison with $P < 0.05$ was considered to be statistically significant. All the analysis was performed in triplicate.

3. Results and discussion

3.1. Elution and purification

The adsorption and desorption rates of MPP in different resins were shown in Fig. 1. The adsorption rates of HPD300, AB-8, and NKA-9 were 92.1 ± 0.7%, 91.8 ± 0.6%, and 74.6 ± 0.2%, suggesting that HPD300 and AB-8 had a far greater adsorption efficiency than that of NKA-9 ($P < 0.05$). The desorption rate of NKA-9 was 92.1 ± 0.4%, which was much higher than that of HPD300 (75.1 ± 0.6%) and AB-8 (73.7 ± 4.4%). Comprehensively, HPD300 was used for the purification of MPP in the current study.

The ethanol concentration of the eluent greatly affected the composition of the components in the eluate (Chen et al., 2016). To disclose the comprehensive profiles of phenolic compounds from mangosteen pericarp, the crude extracts were refined using an HPD300 column, and various eluates were obtained by employing ethanol solutions at 20%, 40%, 60%, or 80% (v/v) concentration. TPC for these four fractions was then determined. The greatest TPC was found in $MPP_{60\%}$ (623 mg/g), which was followed by MPP eluted by the 40% ethanol solution ($MPP_{40\%}$, 589 mg/g), MPP eluted by the 80% ethanol solution ($MPP_{80\%}$, 543 mg/g), and MPP eluted by the 20% ethanol solution ($MPP_{20\%}$, 326 mg/g). Polyphenols from apple pomace were also separated with gradient ethanol elution and HPLC analysis revealed that the majority of the polyphenols were present in fractions eluted between 40% and 50% aqueous ethanol (Cao et al., 2009). We proposed that MPP could be effectively purified by gradient elution with different ethanol concentrations, and the 60% ethanol solution had the best elution effect.

3.2. Qualitative and quantitative analysis

The crude extract (MPP) and these four purified fractions ($MPP_{20\%}$, $MPP_{40\%}$, $MPP_{60\%}$, and $MPP_{80\%}$) were subjected to UPLC-TOF-MS/MS for identification and quantitation of individual phenolic. A total of twenty nine phenolic components were found, including two procyanidins, five flavanols, three phenol acids, one anthocynidin, one flavonoid, and seventeen xanthones. The quantitation data of the phenolic compounds in MPP, $MPP_{20\%}$, $MPP_{40\%}$, $MPP_{60\%}$, and $MPP_{80\%}$ was shown in Table 1. The major procyanidins in mangosteen pericarps were procyanidins B1 and B2, in particular, procyanidins B2 accounted for about 86% of the total procyanidins in tested samples except in $MPP_{20\%}$. The content of procyanidins B2 in $MPP_{20\%}$ was only 788 μg/g, accounting for 0.05% of the total procyanidins. In addition, procyanidin B2 was the most abundant component among the detected components in MPP. Procyanidins B1 was mainly enriched in $MPP_{60\%}$ followed by $MPP_{80\%}$. The identified anthocynidin and flavonoid were cyanidin and luteolin, respectively. Among the flavonols, catechin accounted for 72% of the total flavonols. The contents of catechin in MPP, $MPP_{20\%}$, $MPP_{40\%}$, $MPP_{60\%}$, and $MPP_{80\%}$ were 21.56, 22.51, 29.11, 30.02, and 32.18 mg/g, respectively. Rutin, epicatechin, quercetin glucoside, and taxifolin were also found in low amounts in each sample. Phenolic acids in mangosteen pericarps were mainly salicylic acid, gallic acid, and coumaric acid, while *p*-coumaric acid (58.88 μg/g) was only found in $MPP_{20\%}$. The most abundant phenolic compounds in mangosteen pericarps were xanthones, which were mainly enriched in MPP. Alpha-mangostin, β-mangostin, and gamma (γ)-mangostin were the main components in MPP with a quantity of 8615.93, 79.89, and 2738.35 μg/g, respectively. Only twenty-one main components were found by UPLC-ESI-QTOF-MS/MS in polyphenols extracted with HCl aqueous from mangosteen pericarp (Li et al., 2022). Polyphenol profiles showed remarkable differences due to

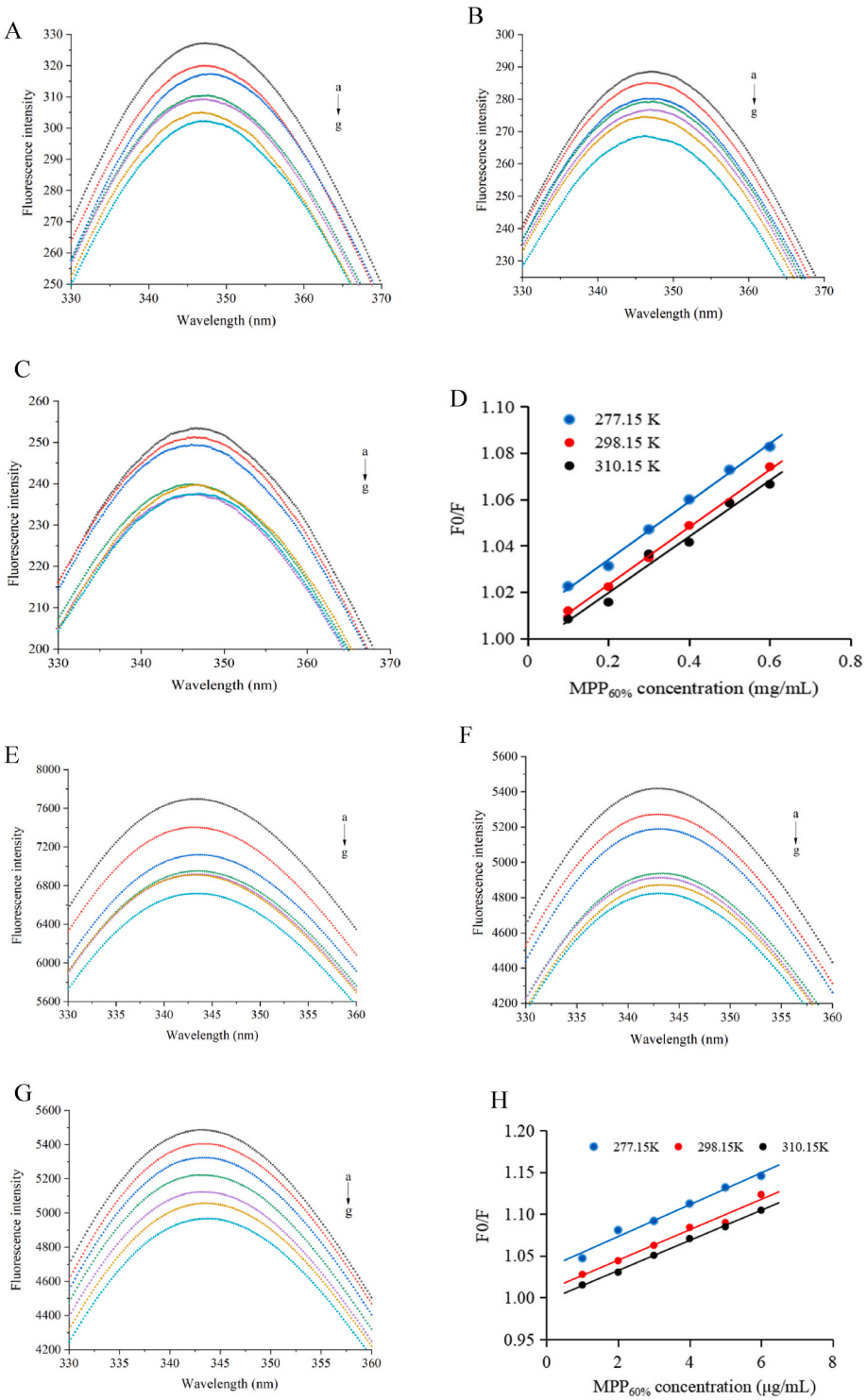

Fig. 4. Fluorescence quenching of α-amylase and α-glucosidase by $MPP_{60\%}$ at different temperatures. (A) 277.15 K for α-amylase. (B) 298.15 K for α-amylase. (C) 310.15 K for α-amylase. (D) Stern-Volmer plots for α-amylase. (E) 277.15 K for α-glucosidase. (F) 298.15 K for α-glucosidase. (G) 310.15 K for α-glucosidase. (H) Stern-Volmer plots for α-glucosidase. The concentrations of $MPP_{60\%}$ to α-amylase were (a) black line, 0 μg/mL (b) red line, 50 μg/mL (c) blue line, 100 μg/mL (d) green line, 125 μg/mL (e) purple line, 150 μg/mL (f) yellow line, 200 μg/mL (g) cyan line, 250 μg/mL. The concentrations of $MPP_{60\%}$ to α-glucosidase were (a) black line, 0 μg/mL (b) red line, 1 μg/mL (c) blue line, 2 μg/mL (d) green line, 3 μg/mL (e) purple line, 4 μg/mL (f) yellow line, 5 μg/mL (g) cyan line, 6 μg/mL. (For interpretation of the references to colour in this figure legend, the reader is referred to the Web version of this article.)

the variations of solvents. It was reported that the acetone-acid system was able to obtain more compositions of polyphenols than the simple acid system (Li et al., 2017a), this could be the reason why more phenolic chemicals were identified in our samples.

Most of the phenolic compounds were consistently found in $MPP_{60\%}$ and $MPP_{80\%}$. A few components were enriched in only one ethanol eluent, for example, coumaric acid was only found in the $MPP_{20\%}$, 1,3,7-trihydroxy-2-(3-methylbut-2-enyl) -xanthone and 1,7-dihydroxy-2-(3-methylbut-2-enyl) -3-methoxyxanthone were enriched in MPP and $MPP_{20\%}$. Hence, phenolic compounds from mangosteen pericarp

Table 3
Binding constants of interaction between $MPP_{60\%}$ and α-amylase/α-glucosidase.

Enzyme	T_m (K)	Regression equation	K_{sv} (L·mg^{-1})	K_q (L·mg^{-1} s^{-1})
α-amylase	277.15	$y = 0.1254x + 1.008$ ($R^2 = 0.995$)	0.1254	0.4222×10^8
	298.15	$y = 0.1240x + 0.998$ ($R^2 = 0.997$)	0.1240	0.4175×10^8
	310.15	$y = 0.1212x + 0.995$ ($R^2 = 0.980$)	0.1212	0.4081×10^8
α-glucosidase	277.15	$y = 0.0200x + 1.029$ ($R^2 = 0.993$)	0.0200	0.0200×10^{11}
	298.15	$y = 0.0193x + 1.006$ ($R^2 = 0.998$)	0.0193	0.0193×10^{11}
	310.15	$y = 0.0180x + 0.996$ ($R^2 = 0.998$)	0.0180	0.0180×10^{11}

Table 4
Pearson correlation coefficients (r) for chemical composition and bioactive capacities of $MPP_{60\%}$.

Phenolic components	*r* value	
	α-glucosidase	α-amylase
procyanidin B1	0.891	0.893
procyanidin B2	−0.886	−0.881
catechin	−0.532	−0.524
epicatechin	0.612	0.615
dihydroquercetin	0.164	0.177
quercetin glucoside	−0.763	−0.761
rutin	0.027	0.101
salicylic acid	0.157	0.153
gallic acid	−0.543	−0.539
cyanidin	0.991	0.990
luteolin	0.126	0.178
α-mangostin	−0.247	−0.254
β-mangostin	−0.497	−0.497
garcinone C	0.993	0.994
mangostanin	−0.997	−0.999
garcinoxanthone D or E	−0.542	−0.449
9-hydroxycalabaxanthone or garcimangosone B	−0.495	−0.500
1,3,6,7-tetrahydroxy-8-prenylxanthone	−0.294	−0.300
1,3,8-trihydroxy-2-(3-methyl-2-butenyl) -4-(3-hydroxy-3-methylbutanoyl)-xanthone	0.935	0.938
1, 2-dihydro-1, 8, 10-trihydroxy-2-(2-hydroxypropan-2-yl) -9-(3-methylbut-2-enyl) furo [3, 2-α] xanthen-11-one	−0.531	−0.438
γ-mangostin	−0.244	−0.251
cudraxanthone G	0.388	0.389
calocalabaxanthone	−0.501	−0.500
garcinone E	−0.241	−0.250

extracts could be effectively separated by using gradient ethanol eluent.

3.3. Inhibitory effects on α-amylase and α-glucosidase

The inhibitory effects of MPP on α-amylase/α-glucosidase were in a dose-dependent manner. The half maximal inhibitory concentration (IC_{50}) values of MPP against α-amylase/α-glucosidase were presented in Table 2. Results showed that the IC_{50} values of MPP, $MPP_{20\%}$, $MPP_{40\%}$, $MPP_{60\%}$ and $MPP_{80\%}$ to α-amylase were 362.6 ± 4.4, 2023.1 ± 10.0, 504.2 ± 16.8, 290.1 ± 4.9 and 1377.0 ± 53.7 μg/mL, respectively. The IC_{50} of acarbose to α-amylase was 49.9 ± 2.7 μg/mL. Adnyana et al. (2016) also reported that the α-amylase inhibition activity of mangosteen pericarps crude extract (extracted by reflux method in 50% ethanol) was much lower than that of acarbose. Given that $MPP_{60\%}$ had the strongest inhibitory effect than other eluted fractions, we assumed that the phenolic compounds in $MPP_{60\%}$ were mainly responsible for the inhibitory effects on α-amylase. The IC_{50} values of MPP, $MPP_{20\%}$, $MPP_{40\%}$, $MPP_{60\%}$ and $MPP_{80\%}$ to α-glucosidase were 7.81 ± 0.69, 31.14 ± 1.78, 6.11 ± 0.07, 6.20 ± 0.15 and 15.21 ± 1.20 μg/mL, which were much lower than that of acarbose against α-glucosidase (53.35 ± 5.44 μg/mL). Apparently, $MPP_{40\%}$ and $MPP_{60\%}$ exhibited superior inhibitory activities on α-glucosidase compared to other eluted fractions. Thus, $MPP_{60\%}$ was selected for additional research on the mechanisms of inhibition because of its superior inhibitory effects on α-amylase and α-glucosidase.

Numerous studies have reported that plant polyphenols exerted inhibitory effects on human carbohydrate digestive enzymes (Ćorković et al., 2022). For instance, phenolic compounds from diverse food resources were effective inhibitors of α-amylase and α-glucosidase, including mulberry fruit (Wattanathorn et al., 2019), cagaita (Daza et al., 2017), cinnamon (Souza et al., 2017), blue pea petal (Pasukamonset et al., 2016) and purple sweet potato (Yang et al., 2021). The inhibitory effect of dietary polyphenols on α-amylase and α-glucosidase contributed to the retarded starch digestion and diminished postprandial hyperglycemia. Therefore, polyphenols from mangosteen pericarp might be created as functional foods to prevent or alleviate type 2 diabetes.

3.4. Lineweaver-Burk, Dixon and Cornish-Bowden plots

The inhibition kinetics of $MPP_{60\%}$ to α-amylase/α-glucosidase were investigated by Lineweaver-Burk, Dixon, and Cornish-Bowden plots in this study. In general, there are three categories of reversible inhibitions including competitive inhibition, non-competitive inhibition, and uncompetitive inhibition (Sun et al., 2019). As displayed in Fig. 2, for α-amylase, lines intersected in the first quadrant (close to the y-axis) in the Lineweaver-Burk plot (Fig. 2A). In addition, lines ran parallel with each other in the Cornish-Bowden plot (Fig. 2B), and showed clear intersection points in the Dixon plot (Fig. 2C). The results indicated that the inhibitory type of $MPP_{60\%}$ on α-amylase was a competitive inhibition, and the K_{ic} was 125.54 ± 4.41 μg/mL. For α-glucosidase, all lines were fitted and intersected in the second quadrant in the Lineweaver–Burk plot (Fig. 2D), both Dixon (Fig. 2E) and Cornish-Bowden (Fig. 2F) lines intersected at a single point, suggesting that the inhibition of $MPP_{60\%}$ against α-glucosidase was a mixed-type inhibition. Calculation results showed that the K_{ic} and K_{iu} were 6.30 ± 0.04 μg/mL and 2.50 ± 0.02 μg/mL, respectively. The results indicated that $MPP_{60\%}$ could not only compete with α-glucosidase for the active *p*NPG-binding site(s) but also bind with α-glucosidase-*p*NPG inclusion complex in uncompetitive mode.

However, Li and colleagues found that the inhibitory effect of polyphenols extracted with HCl aqueous from mangosteen pericarp on α-amylase was a non-competitive inhibition (Li et al., 2022). Actually, several parameters may affect the inhibition activities of polyphenol extract on α-amylase and α-glucosidase, including sample preparation, sample pretreatment, extraction technique, solvent type, and purification method. The molecular structures of polyphenols also influenced their inhibitory effects to α-amylase/α-glucosidase (Xiao et al., 2013; Ćorković et al., 2022). Therefore, polyphenols derived from the same raw material could show varying levels of inhibitory activity against α-amylase and α-glucosidase.

3.5. CD analysis

The corresponding CD spectrum may show the changes in the structure of enzymes (He et al., 2021; Zheng et al., 2020). Therefore, the current investigation predicted the proportional contents of α-helix, β-sheet, β-turn, and random coil in α-amylase and α-glucosidase by CD spectrum. The contents of the random coil and β-turn exhibited increasing trends, while the contents of the α-helix and β-sheet showed decreasing trends. The amount of β-sheet was 51.5% for α-amylase without the addition of $MPP_{60\%}$, and it decreased to 50.6% in the presence of 250 μg/mL $MPP_{60\%}$. On the contrary, the β-turn content for α-amylase was 16.8% without the existence of $MPP_{60\%}$, and it increased to 17.7% in the presence of 250 μg/mL $MPP_{60\%}$ (Fig. 3A). For α-glucosidase, α-helix content decreased from 8.2% to 5.5% and β-sheet content

decreased from 49.3% to 31.2% with the inclusive of $MPP_{60\%}$. In addition, β-turn content increased from 18.2% to 20.2%, and random coil content increased from 28.8% to 38.6% (Fig. 3B). The findings suggested that both α-amylase and α-glucosidase underwent modifications in their secondary structures due to the effects of $MPP_{60\%}$. From the perspective of numerical changes, the impact of $MPP_{60\%}$ on α-glucosidase was greater than that on α-amylase, which might be due to the binding sites of $MPP_{60\%}$ in enzymes. Molecular docking proved that the binding sites of flavonoids in α-amylase and α-glucosidase were different and various hydrogen bonds were formed (Tian et al., 2021). Therefore, we speculated that the hydrogen bonds and hydrophobic action of the enzymes might be changed by $MPP_{60\%}$, which hindered the active site formation or prevented substrate binding and subsequently affected the activity of these enzymes (Wu et al., 2018).

3.6. Fluorescence quenching analysis

Fluorescence quenching experiments were conducted at different temperatures (277.15 K, 298.15 K, and 310.15 K) to further examine the interaction between α-amylase/α-glucosidase and $MPP_{60\%}$. The fluorescence spectra of α-amylase and α-glucosidase were displayed in Fig. 4. The maximum emission wavelength was 347.2 nm for α-amylase (Fig. 4A–C) and 344.2 nm for α-glucosidase (Fig. 4E–G) at excitation of 280 nm. The fluorescence intensity of α-amylase/α-glucosidase decreased with the increased $MPP_{60\%}$ concentration, indicating that the endogenous fluorescence of the enzymes was quenched by $MPP_{60\%}$. However, fluorescence quenching occurred without a significant peak shift. As previously reported, aromatic amino acids including tyrosine, tryptophan, and phenylalanine were primarily responsible for the endogenous fluorescence of α-amylase/α-glucosidase (Deng et al., 2011; Han et al., 2017). Consequently, it is possible that $MPP_{60\%}$ directly interacted with the aromatic amino acids, which in turn caused the quenching of fluorescence.

Stern-Volmer parameters were used to clear the fluorescence quenching mechanism. Fluorescence quenching can be categorized as static quenching, dynamic quenching, or a mixed type of both, the first mechanism forms a non-fluorescent complex between the fluorophore and the quencher, while the second is induced by energy collision (Peng et al., 2016). Fig. 4D and H showed the Stern-Volmer plots of fluorescence quenching of α-amylase and α-glucosidase induced by $MPP_{60\%}$ at different temperatures. A strong linear correlation was seen among all the Stern-Volmer curves, indicating that there was a single type of interaction occurring between quencher and α-amylase/α-glucosidase. The fluorescence quenching rate constant K_q and K_{sv} of the samples calculated through Stern-Volmer plots were shown in Table 3. The K_q value for α-amylase (0.4222×10^8 L mg^{-1} s^{-1}, 0.4175×10^8 L mg^{-1} s^{-1} and 0.4081×10^8 L mg^{-1} s^{-1} for 277.15 K, 298.15 K and 310.15 K, respectively) and α-glucosidase (0.0200×10^{11} L mg^{-1} s^{-1}, 0.0193×10^{11} L mg^{-1} s^{-1} and 0.0180×10^{11} L mg^{-1} s^{-1} for 277.15 K, 298.15 K and 310.15 K, respectively) decreased as the temperature increased from 277.15 K to 310.15 K, indicating that the fluorescence quenching of $MPP_{60\%}$ to α-amylase/α-glucosidase was a static quenching (Tong, Zhu, Guo, Peng, & Zhou, 2018).

3.7. Pearson correlation coefficient analysis

Pearson correlation is the most commonly used correlation analysis, and Pearson correlation coefficients (r) describe the degree of correlation between two variables. To establish the relationships between phenolic compositions and functionality of polyphenols from mangosteen pericarp. The correlation analysis between chemical composition in $MPP_{60\%}$ and inhibitory effects to α-amylase/α-glucosidase (IC_{50}) was performed using Pearson correlation coefficients, and r value represented the strength of the correlation. Results presented in Table 4 showed that procyanidin B2 ($r = -0.881$), quercetin glucoside ($r = -0.761$), and mangostanin ($r = -0.999$) were the main functional phenolics in $MPP_{60\%}$ that inhibited α-amylase activity. Similarly, procyanidin B2 ($r = -0.886$), quercetin glucoside ($r = -0.763$), and mangostanin ($r = -0.997$) were also presented as the main phenolic components associated with the α-glucosidase inhibition activity. The high correlation between the biological activity of $MPP_{60\%}$ and procyanidin B2 may be attributed to the high content of procyanidin B2 in $MPP_{60\%}$. Procyanidins ($r = -0.75$) were also reported to have mainly involved in α-amylase and α-glucosidase inhibitory activity in polyphenol-rich extracts of six analyzed bean cultivars (Ombra et al., 2018). Given the strong link, we anticipated that $MPP_{60\%}$ would include a significant amount of mangostanin. On the other hand, a median quantity of mangostanin was found in $MPP_{60\%}$, suggesting that the inhibition of a-amylase/α-glucosidase ought to rely more on a mix of several substances.

4. Conclusions

In summary, the comprehensive phenolic profile of mangosteen pericarp was revealed by gradient ethanol elution and UPLC-Q-TOF-MS/MS. A total of twenty nine phenolic compounds were identified and quantified. $MPP_{60\%}$ showed the highest TPC (623 mg/g) and presented effective inhibitory activity on α-amylase and α-glucosidase with the IC_{50} values of 290.1 ± 4.9 μg/mL and 6.20 ± 0.15 μg/mL. Moreover, the inhibition of $MPP_{60\%}$ on α-amylase was a competitive inhibition with K_{ic} of 125.54 ± 4.41 μg/mL, while the inhibition on α-glucosidase was a mixed-type inhibition with uncompetitive inhibition stronger than competitive inhibition. The K_{ic} and the K_{iu} were 6.30 ± 0.04 μg/mL and 2.50 ± 0.02 μg/mL, respectively. The inhibitory effects could be attributed to the changes in the secondary structure as well as the static fluorescence quenching of the enzymes induced by $MPP_{60\%}$ treatment. In addition, Pearson correlation coefficients revealed that procyanidin B2, quercetin glucoside, and mangostain contributed most to inhibiting α-amylase and α-glucosidase activity. The above findings indicated that phenolic compounds from mangosteen pericarp can potentially be developed into the inhibitors of α-amylase/α-glucosidase for type 2 diabetes treatment.

CRediT authorship contribution statement

Mengting Lai: Software, Methodology, Formal analysis, Conceptualization. **Hongzhu Chen:** Writing – original draft, Software, Methodology, Formal analysis, Conceptualization. **Xiaozhen Liu:** Writing – review & editing, Supervision, Project administration, Funding acquisition, Conceptualization. **Fuxiang Li:** Writing – original draft, Software, Methodology. **Fengyuan Liu:** Writing – review & editing, Conceptualization. **Yuting Li:** Writing – review & editing. **Jingkun Yan:** Writing – review & editing, Supervision. **Li Lin:** Supervision, Funding acquisition.

Declaration of competing interest

The authors confirm that they have no conflicts of interest with respect to the work described in this manuscript.

Data availability

Data will be made available on request.

Acknowledgements

We sincerely thank the following organizations for providing financial support for this work: the National Natural Science Foundation of China (81803193), the Institute of Science and Technology Innovation, Dongguan University of Technology, China (KCYCXPT2017007), and Foundation for Innovation Team in Higher Education of Guangdong, China (2021KCXTD035). In addition, the authors acknowledge the assistance of Dongguan University of Technology Analytical and Testing

Center.

References

Adnyana, I. K., Abuzaid, A. S., Iskandar, E. Y., & Kurniati, N. F. (2016). Pancreatic lipase and α-amylase inhibitory potential of mangosteen (*Garcinia mangostana Linn.*) pericarp extract. *International Journal of Medical Research & Health Sciences, 5*(1), 23–28. https://doi.org/10.5958/2319-5886.2016.00006.0

Cao, H., Ou, J., Chen, L., Zhang, Y., Szkudelski, T., Delmas, D., Daglia, M., & Xiao, J. (2018). Dietary polyphenols and type 2 diabetes: Human study and clinical trial. *Critical Reviews in Food Science and Nutrition, 59*(20), 3371–3379. https://doi.org/10.1080/10408398.2018.1492900

Cao, X., Wang, C., Pei, H., & Sun, B. (2009). Separation and identification of polyphenols in apple pomace by high-speed counter-current chromatography and high-performance liquid chromatography coupled with mass spectrometry. *Journal of Chromatography A, 1216*(19), 4268–4274. https://doi.org/10.1016/j.chroma.2009.01.046

Chandra, A., Rana, J., & Li, Y. (2001). Separation, identification, quantification, and method validation of anthocyanins in botanical supplement raw materials by HPLC and HPLC-MS. *Journal of Agricultural and Food Chemistry, 49*(8), 3515–3521. https://doi.org/10.1021/jf010389p

Chen, X., He, X., Zhang, B., Sun, L., Liang, Z., & Huang, Q. (2019). Wheat gluten protein inhibits α-amylase activity more strongly than a soy protein isolate based on kinetic analysis. *International Journal of Biological Macromolecules, 129*, 433–441. https://doi.org/10.1016/j.ijbiomac.2019.01.215

Chen, Y., Zhang, W., Zhao, T., Li, F., Zhang, M., Li, J., Zou, Y., Wang, W., Cobbina, S. J., & Wu, X. (2016). Adsorption properties of macroporous adsorbent resins for separation of anthocyanins from mulberry. *Food Chemistry, 194*, 712–722. https://doi.org/10.1016/j.foodchem.2015.08.084

Ćorković, I., Gašo-Sokač, D., Pichler, A., Šimunović, J., & Kopjar, M. (2022). Dietary polyphenols as natural inhibitors of α-amylase and α-glucosidase. *Life, 12*(11), 1692–1700. https://doi.org/10.3390/life12111692

Croft, K. D. (2016). Dietary polyphenols: Antioxidants or not? *Archives of Biochemistry and Biophysics, 595*, 120–124. https://doi.org/10.1016/j.abb.2015.11.014

Daza, L. D., Fujita, A., Granato, D., Fávaro-Trindade, C. S., & Inés Genovese, M. (2017). Functional properties of encapsulated Cagaita (*Eugenia dysenterica DC.*) fruit extract. *Food Bioscience, 18*, 15–21. https://doi.org/10.1016/j.fbio.2017.03.003

Deng, Y. F., Aluko, R. E., Jin, Q., Zhang, Y., & Yuan, L. J. (2011). Inhibitory activities of baicalin against renin and angiotensin-converting enzyme. *Pharmaceutical Biology, 50*(4), 401–406. https://doi.org/10.3109/13880209.2011.608076

Eisenthal, R., & Cornish-Bowden, A. (1974). The direct linear plot. A new graphical procedure for estimating enzyme kinetic parameters. *Biochemical Journal, 139*(3), 715–720. https://doi.org/10.1042/bj1390715

Ghasemzadeh, A., Jaafar, H., Baghdadi, A., & Tayebi-Meigooni, A. (2018). Alpha-mangostin-rich extracts from mangosteen pericarp: Optimization of green extraction protocol and evaluation of biological activity. *Molecules, 23*(8), 1852. https://doi.org/10.3390/molecules23081852

Han, L., Fang, C., Zhu, R., Peng, Q., Li, D., & Wang, M. (2017). Inhibitory effect of phloretin on α-glucosidase: Kinetics, interaction mechanism and molecular docking. *International Journal of Biological Macromolecules, 95*, 520–527. https://doi.org/10.1016/j.ijbiomac.2016.11.089

Han, L., Wang, H., Cao, J., Jin, X., He, C., Wang, M., & Li, Y. (2023). Inhibition mechanism of α-glucosidase inhibitors screened from Tartary buckwheat and synergistic effect with acarbose. *Food Chemistry, 420*, Article 136102. https://doi.org/10.1016/j.foodchem.2023.136102

He, T., Zhao, L., Chen, Y., Zhang, X., Hu, Z., & Wang, K. (2021). Longan seed polyphenols inhibit α-amylase activity and reduce postprandial glycemic response in mice. *Food & Function, 12*(24), 12338–12346. https://doi.org/10.1039/d1fo02891j

Hossain, U., Das, A. K., Ghosh, S., & Sil, P. C. (2020). An overview on the role of bioactive α-glucosidase inhibitors in ameliorating diabetic complications. *Food and Chemical Toxicology, 145*, Article 111738. https://doi.org/10.1016/j.fct.2020.111738

Janeček, Š., Svensson, B., & Macgregor, E. A. (2014). α-Amylase: An enzyme specificity found in various families of glycoside hydrolases. *Cellular and Molecular Life Sciences, 71*(7), 1149–1170. https://doi.org/10.1007/s00018-013-1388-z

Karas, M., Jakubczyk, A., Szymanowska, U., Złotek, U., & Zielińska, E. (2016). Digestion and bioavailability of bioactive phytochemicals. *International Journal of Food Science and Technology, 52*(2), 291–305. https://doi.org/10.1111/ijfs.13323

Li, X., Chen, H., Jia, Y., Peng, J., & Li, C. (2022). Inhibitory effects against alpha-amylase of an enriched polyphenol extract from pericarp of mangosteen. *Foods, 11*(7), 1001–1017. https://doi.org/10.3390/foods11071001

Li, F., Zhang, B., Chen, G., & Fu, X. (2017a). Analysis of solvent effects on polyphenols profile, antiproliferative and antioxidant activities of mulberry (*Morus alba L.*) extracts. *International Journal of Food Science and Technology, 52*(7), 1690–1698. https://doi.org/10.1111/ijfs.13443

Li, F., Zhang, B., Chen, G., & Fu, X. (2017b). The novel contributors of anti-diabetic potential in mulberry polyphenols revealed by UHPLC-HR-ESI-TOF-MS/MS. *Food Research International, 100*, 873–884. https://doi.org/10.1016/j.foodres.2017.06.052

Lim, Y. K., Yoo, S. Y., Jang, Y. Y., Lee, B. C., Lee, D. S., & Kook, J. K. (2020). Anti-inflammatory and in vitro bone formation effects of *Garcinia mangostana L.* and propolis extracts. *Food Science and Biotechnology, 29*(4), 539–548. https://doi.org/10.1007/s10068-019-00697-3

Luca, S. V., Macovei, I., Bujor, A., Miron, A., Skalicka-Woniak, K., Aprotosoaie, A. C., & Trifan, A. (2020). Bioactivity of dietary polyphenols: The role of metabolites. *Critical Reviews in Food Science and Nutrition, 60*(4), 626–659. https://doi.org/10.1080/10408398.2018.1546669

Ombra, M. N., Acierno, A., Nazzaro, F., Spigno, P., Riccardi, R., Zaccardelli, M., Pane, C., Coppola, R., & Fratianni, F. (2018). Alpha-amylase, α-glucosidase and lipase inhibiting activities of polyphenol-rich extracts from six common bean cultivars of Southern Italy, before and after cooking. *International Journal of Food Sciences & Nutrition, 69*(7), 824–834. https://doi.org/10.1080/09637486.2017.1418845

Papoutsis, K., Zhang, J., Bowyer, M. C., Brunton, N. P., & Lyng, J. (2021). Fruit, vegetables, and mushrooms for the preparation of extracts with α-amylase and α-glucosidase inhibition properties: A review. *Food Chemistry, 338*, Article 128119. https://doi.org/10.1016/j.foodchem.2020.128119

Pasukamonset, P., Kwon, O., Adisakwattana, & Sirichai. (2016). Alginate-based encapsulation of polyphenols from *Clitoria ternatea* petal flower extract enhances stability and biological activity under simulated gastrointestinal conditions. *Food Hydrocolloids, 61*, 772–779. https://doi.org/10.1016/j.foodhyd.2016.06.039

Peng, X., Wang, X., Qi, W., Su, R., & He, Z. (2016). Affinity of rosmarinic acid to human serum albumin and its effect on protein conformation stability. *Food Chemistry, 192*, 178–187. https://doi.org/10.1016/j.foodchem.2015.06.109

Prendergast, F. G., Lu, J., & Callahan, P. J. (1983). Oxygen quenching of sensitized terbium luminescence in complexes of terbium with small organic ligands and proteins. *Journal of Biological Chemistry, 258*(7), 4075–4078. https://doi.org/10.1016/S0021-9258(18)32585-7

Rusman, J. R. A., Sundari, S. A., Nuriliani, A., & Saragih, H. T. (2021). Ameliorative effect of Mangosteen (*Garcinia mangostana L.*) peel infusion on the histopathological structures of the liver and kidney of rats (*Rattus norvegicus* Berkenhout, 1769) after H_2O_2 induction. *Veterinary World, 14*(6), 1579–1587. https://doi.org/10.14202/vetworld.2021.1579-1587

Souza, V. B. D., Thomazini, M., Barrientos, M. A. E., Nalin, C. M., Ferro-Furtado, R., Genovese, M. I., & Favaro-Trindade, C. S. (2017). Functional properties and encapsulation of a proanthocyanidin-rich cinnamon extract (*Cinnamomum zeylanicum*) by complex coacervation using gelatin and different polysaccharides. *Food Hydrocolloids, 77*, 297–306. https://doi.org/10.1016/j.foodhyd.2017.09.040

Stefek, M. (2011). Natural flavonoids as potential multifunctional agents in prevention of diabetic cataract. *Interdisciplinary Toxicology, 4*(2), 69–77. https://doi.org/10.2478/v10102-011-0013-y

Sun, H., Saeedi, P., Karuranga, S., Pinkepank, M., Ogurtsova, K., Duncan, B. B., Stein, C., Basit, A., Chan, J. C. N., & Mbanya, J. C. (2022). IDF Diabetes Atlas: Global, regional and country-level diabetes prevalence estimates for 2021 and projections for 2045. *Diabetes Research and Clinical Practice, 183*, Article 109119. https://doi.org/10.1016/j.diabres.2021.109119

Sun, L., Warren, F. J., & Gidley, M. (2019). Natural products for glycaemic control: Polyphenols as inhibitors of alpha-amylase. *Trends in Food Science & Technology, 91*, 262–273. https://doi.org/10.1016/j.tifs.2019.07.009

Sun, L., Warren, F. J., Netzel, G., & Gidley, M. (2016). 3 or 3′-Galloyl substitution plays an important role in association of catechins and theaflavins with porcine pancreatic α-amylase: The kinetics of inhibition of α-amylase by tea polyphenols. *Journal of Functional Foods, 26*, 144–156. https://doi.org/10.1016/j.jff.2016.07.012

Tian, J., Si, X., Wang, Y., Gong, E., Xie, X., Zhang, Y., Li, B., & Shu, C. (2021). Bioactive flavonoids from *Rubus corchorifolius* inhibit α-glucosidase and α-amylase to improve postprandial hyperglycemia. *Food Chemistry, 341*, Article 128149. https://doi.org/10.1016/j.foodchem.2020.128149

Tinajero, M. G., & Malik, V. S. (2021). An update on the epidemiology of type 2 diabetes: A global perspective. *Endocrinology and Metabolism Clinics of North America, 50*, 337–355. https://doi.org/10.1016/j.ecl.2021.05.013

Tong, D. P., Zhu, K. X., Guo, X. N., Peng, W., & Zhou, H. M. (2018). The enhanced inhibition of water extract of black tea under baking treatment on α-amylase and α-glucosidase. *International Journal of Biological Macromolecules, 107*, 129–136. https://doi.org/10.1016/j.ijbiomac.2017.08.152

Wattanathorn, J., Kawvised, S., & Thukham-Mee, W. (2019). Encapsulated mulberry fruit extract alleviates changes in an animal model of menopause with metabolic syndrome. *Oxidative Medicine and Cellular Longevity, 2019*(3), 1–23. https://doi.org/10.1155/2019/5360560

Wihastuti, T. A., Aini, F. N., Tjahjono, C. T., & Heriansyah, T. (2019). Dietary ethanolic extract of mangosteen pericarp reduces VCAM-1, perivascular adipose tissue and aortic intimal medial thickness in hypercholesterolemic rat model. *Open Access Macedonian Journal of Medical Sciences, 7*(19), 3158–3163. https://doi.org/10.3889/oamjms.2019.717

Wu, X., Ding, H., Hu, X., Pan, J., & Liao, Y. (2018). Exploring inhibitory mechanism of gallocatechin gallate on a-amylase and a-glucosidase relevant to postprandial hyperglycemia. *Journal of Functional Foods, 48*, 200–209. https://doi.org/10.1016/j.jff.2018.07.022

Xiao, J., & Högger, P. (2015). Dietary polyphenols and type 2 diabetes: Current insights and future perspectives. *Current Medicinal Chemistry, 22*(1), 23–38. https://doi.org/10.2174/0929867321666140706130807

Xiao, J., Ni, X., Kai, G., & Chen, X. (2013). A review on structure-activity relationship of dietary polyphenols inhibiting α-amylase. *Critical Reviews in Food Science and Nutrition, 53*(5), 497–506. https://doi.org/10.1080/10408398.2010.548108

Yan, Y., Wu, T., Zhang, M., Li, C., Liu, Q., & Li, F. (2022). Prevalence, awareness and control of type 2 diabetes mellitus and risk factors in Chinese elderly population. *BMC Public Health, 22*(1), 1382. https://doi.org/10.1186/s12889-022-13759-9

Yang, Y., Zhang, J. L., Shen, L. H., Feng, L. J., & Zhou, Q. (2021). Inhibition mechanism of diacylated anthocyanins from purple sweet potato (*Ipomoea batatas L.*) against α-amylase and α-glucosidase. *Food Chemistry, 359*, Article 129934. https://doi.org/10.1016/j.foodchem.2021.129934

Zhang, X., Li, G.l., Wu, D., Yu, Y., Hu, N., Wang, H., Li, X., & Wu, Y. (2020). Emerging strategies for the activity assay and inhibitor screening of alpha-glucosidase. *Food & Function, 11*(1), 66–82. https://doi.org/10.1039/c9fo01590f

Zhang, L., Tu, Z. C., Yuan, T., Wang, H., Xie, X., & Fu, Z. F. (2016). Antioxidants and α-glucosidase inhibitors from Ipomoea batatas leaves identified by bioassay-guided approach and structure-activity relationships. *Food Chemistry, 208*, 61–67. https://doi.org/10.1016/j.foodchem.2016.03.079

Zheng, R., Su, S., Zhou, H., Yan, H., Ye, J., Zhao, Z., You, L., & Fu, X. (2017). Antioxidant/antihyperglycemic activity of phenolics from sugarcane (*Saccharum officinarum L.*) bagasse and identification by UHPLC-HR-TOFMS. *Industrial Crops and Products, 101*, 104–114. https://doi.org/10.1016/j.indcrop.2017.03.012

Zheng, Y., Tian, J., Yang, W., Chen, S., & Ye, X. (2020). Inhibition mechanism of ferulic acid against α-amylase and α-glucosidase. *Food Chemistry, 317*, Article 126346. https://doi.org/10.1016/j.foodchem.2020.126346